Synthesis of hydrous iron oxide/aluminum hydroxide composite loaded on coal fly ash as an effective mesoporous and low-cost sorbent for Cr (VI) sorption: Fuzzy Logic Modeling

Seyed Mostafa Hosseini Asl[a], Mojtaba Masomi[a], Morteza Hosseini[b], Hamedreza Javadian[c,*], Montserrat Ruiz[d], Ana Maria Sastre[c]

[a]Ayatollah Amoli Branch, Department of Chemical Engineering, Islamic Azad University, Amol, Iran

[b]Faculty of Chemical Engineering, Babol Noshirvani University of Technology, P. O. Box 484, Shariati St., Babol 4714871167, Iran

[c]Universitat Politècnica de Catalunya, Department of Chemical Engineering, ETSEIB, Diagonal 647, 08028 Barcelona, Spain

[d]Universitat Politècnica de Catalunya, Department of Chemical Engineering, EPSEVG, Av. Víctor Balaguer, s/n, 08800 Vilanova i la Geltrú, Spain

[*]Corresponding author: Hamedreza Javadian, Universitat Politècnica de Catalunya, Department of Chemical Engineering, ETSEIB, Diagonal 647, 08028 Barcelona, Spain

E-mail addresses: hamedreza.javadian@upc.edu; hamedreza.javadian@yahoo.com (H. Javadian)

Abstract

The aim of this research was to estimate the possibility of using synthesized hydrous iron oxide/aluminium hydroxide composite loaded on coal fly ash (FA3) as an efficient sorbent for Cr (VI) sorption from aqueous solution. In this regard, dissolution and precipitation processes were performed to rearrange and load the intrinsic iron and aluminum on the surface of fly ash. Different characterization techniques including XRD, XRF, FT-IR, SEM, LPS and BET surface area were applied to analyze the sorbent properties. Moreover, sorption kinetics were studied using Morris–Weber intra-particle diffusion, Lagergren pseudo-first-order and pseudo-second-order models. The kinetic analyses indicated that pseudo-first-order model controlled the sorption process. In order to estimate the sorbent capacity, Langmuir, Freundlich and D–R models were applied. The thermodynamic parameters of Cr (VI) sorption were also studied. In addition, removal efficiency of Cr (VI) was predicted using the developed fuzzy logic model. The fuzzification of four input variables including pH, contact time, adsorbent dose and initial Cr (VI) concentration versus removal efficiency as output was carried out using an artificial intelligence-based approach. A Mamdani-type fuzzy interface system was employed to fulfill a collection of 24 rules (If-Then format) using triangle membership functions (MF_S) with seven levels in fuzzy sets. The proposed fuzzy logic model demonstrated high predictive performance with correlation coefficient (R^2) of 0.95 and acceptable deviation from the experimental data, confirming its suitability to predict Cr (VI) removal efficiency. Based on experimental data and statistical analysis, the synthetized sorbent was effective for treating wastewater containing Cr (VI).

Keywords: Fly ash, $FeOOH/Al(OH)_3$, Sorption, Cr (VI), Isotherm, Fuzzy logic modeling.

1. Introduction

Considering the role of water and its significance in human health, the decrease in its quality by pollution, and the fact that the common treatment methods are not completely successful for removal of contaminants from wastewaters to meet the standard limits, the introduction of new attitudes and methods seems to be very necessary [1,2]. Nowadays, heavy metals are the most prominent water pollutants that are classified as the biggest threat to the environment and global health. Heavy metal ions are stable and non-biodegradable in the environment, plus having high tendency to be accumulated in living organisms causing serious illnesses. Among all heavy metals, chromium can be found easily on the earth's surface with two common oxidation states of Cr^{+2} and Cr^{+6}. From biological point of view, the toxicity of trivalent and hexavalent chromium are important to human health [2]. The hexavalent chromium Cr (VI) is dangerous for human health causing skin irritation, membranous mucous and special joints with macromolecules [3]. Human exposure to high levels of Cr (VI) may have harmful effects on liver, kidneys, blood, gastrointestinal and immune systems [3]. According to the International Agency for Research on Cancer (IARC), European Union and USA poison detection program [2], hexavalent chromium accompanied by arsenic, beryllium, cadmium and nickel can be a major cause of cancer. The global standard limits of chromium for water and drinking water are 0.1 and 0.05 mg/L, respectively [3], and the maximum concentration of chromium in drinking water reported by the national standard institute of Iran is also 0.05 mg/L.

Various physical and chemical techniques are used to remove heavy metal ions from aqueous solutions, most of which have some disadvantages including chemical precursor demand, high production costs, toxic sludge production and incomplete removal of metals [4-6]. Among all methods, sorption is an effective process considered as an economical and beneficial

method to remove heavy metals from aqueous solutions [7]. In this regard, activated carbon is one of the most commonly used sorbents for treatment of water and wastewater. However, the high application cost has dramatically restricted its widespread use [8]. Therefore, different natural sorbents have been introduced as alternative candidates for sorption of toxic metal ions from aqueous solutions.

Application of coal as a fuel in most industries results in producing high amount of fly ash as by-product that leads to air pollution and disposal problems; therefore, the application and utilization of fly ash seems to be indispensable [7,9]. Adsorption using a variety of iron-containing materials has proven to be easy, economical and effective. Thus, several iron-containing materials such as amorphous hydrous iron oxide (FeOOH), goethite (α-FeOOH) and akaganeite (β-FeOOH) have been examined and proven to be promising adsorptive materials due to their high removal efficiency [10]. Among these materials, amorphous hydrous iron oxide has the highest sorption capability due to its high surface area. However, this iron-containing sorbent is merely available as fine powder or exists as gel or suspension in aqueous solutions. Hence, it is difficult to be separated entirely from treated solution after sorption process [10]. In order to overcome this shortage, some matrices or platforms should be selected to support or load those iron oxides. Studies indicated that synthetic Fe-loaded sorbents based on matrices such as municipal solid waste (MSW), cement, sand, activated alumina (AA), silica oxide and alginate beads had proper affinities for high Cr (VI) removal efficiency. Recently, we have found a new type of coal fly ash with iron oxide and aluminum oxide contents of approximately 18.07 and 28.73 % which seems to be an ideal Fe and Al containing raw material to synthesize an adsorbent for Cr (VI) sorption.

The removal parameters of heavy metals have been broadly modeled using prevalent artificial intelligence techniques such as Adaptive Neural Fuzzy Inference Systems (ANFIS) and Artificial Neural Network (ANN) [11,12]. Fuzzy Inference System (FIS) has also been one of the viable options to predict the removal behavior of sorbent during a sorption process. Fuzzy logic is known as one of the best methods to implement expert knowledge (EK) and establish an advanced monitoring on different treatment processes particularly where there is not applicable software in primary units of a wastewater treatment system as a whole. Since Fuzzy Interface Systems (FIS) doesn't need to analyze the certain and exact information of a process, it has been vastly applied in industrial and commercial control systems [13]. The model-based fuzzy control systems are the latest investigational achievements conducted on fuzzy logic control, exhibiting acceptable stability and performance specifically in closed-loop fuzzy control systems [14]. Fuzzy inference system is composed of membership functions to determine and control variables, produced rules by experienced operators and a fuzzy inference engine [15]. In fact, the main contribution in assessing adsorption processes and finding the best solution for operational problems is the responsibility of professional experts.

The main goal of the present study was to develop a new route for effective utilization of a special type of fly ash to synthesize a novel sorbent containing high amount of FeOOH in a composite form with Al $(OH)_3$ using simple chemical reactions. The sorbent was applied to remove Cr (VI) from aqueous systems at optimum conditions. The experimental data obtained from Cr (VI) sorption were modeled by Fuzzy Inference System (FIS) in order to predict its removal efficiency. Removal efficiency of Cr (VI) as a response was affected by several parameters consisting of pH, contact time, adsorbent dose and Cr (VI) concentration. The effect of each input variable on output variable was determined using sensitivity analysis. Both

empirical data obtained from the measured variables and expert knowledge (EK) were employed into the fuzzy inference system (FIS) with Mamadani method through fuzzy-based rule structure. The satisfactory results of the developed fuzzy logic modeling showed that it can be used to predict the quality of probable effluent in primary treatment units.

1.1. Fuzzy logic modeling

Among different statistical analyses, fuzzy modeling is recognized as a strong technique to estimate the relation between input variables and output response in intricate nonlinear systems. Zadeh expressed that variables help to eliminate uncertainties and have important impacts on fuzzy numbers [16]. In fact, a fuzzy number is responsible to describe available relationship between an uncertain quantity x and a membership function μ changing from zero to one [17]. The fuzzy inference systems are divided into two distinct types including Takagi–Sugeno models [18] and Mamdani models [19]. The relationships between output membership functions and input variables in Takagi-Sugeno models are designed in the form of a constant or linear function, while in Mamdani models, the output membership functions are fuzzy sets in which each linguistic information can incorporate into the model. Researches proved that the qualitative information can be modeled by Mamdani models with acceptable performance [20]. The fundamental section of fuzzy logic is a set of human language rules defined by the user. The procedure of fuzzy systems is the conversion of rules to their mathematical equivalents. Consequently, the industrial designer can easily work with accurate outputs obtained from these systems behaving similar to real conditions. The simplicity and flexibility properties of fuzzy logic are considered as its further benefits. Fuzzy logic not only solves problems regarding inaccurate and imperfect data, but also models nonlinear functions in each level of complexity [21,22]. One advantage of fuzzy logic in comparison with ANNs is the high capability of

handling multivariate data particularly noisy and distorted ones. The major superiority of fuzzy modeling is its training phase where the rules are established even without the presence of accurate data, merely relying on expert knowledge to constitute the rule base. According to relevant investigations, the interpretation of results obtained from fuzzy model and its rules can be comfortably performed in comparison to ANNs [23]. The relationships between the input and output in fuzzy model are described using fuzzy if-then rules (fuzzy propositions). In fact, the fuzzy sets and proximate argumentations help to find an appropriate solution for a specific problem without having required details regarding any domain of knowledge. The expert knowledge plays an important role in the formulation of fuzzy rules [24]. Mamdani design of fuzzy logical model is called linguistic model because each rule is defined based on If-Then relationship, in which both the antecedent and the consequent are fuzzy propositions [25]. The manual development of model structure is carried out without any need to training and optimizing steps for final model. The created rules in a Mamadani model strongly affect the outputs consisting fuzzy membership functions. This generalized model relies on adequate expert knowledge of a system instead of data set that makes it an effective model for future predictions [26]. Linguistic variables such as X, Y and Z in the structure of Mamdani models conform to the rule base as follows:

R_i: if X is A_i and Y is B_i,. . . then Z is C_i,. . ., i = 1. . .n, (x_0, y_0) is determined as an input and the main purpose of the model is the determination of output (Z or C). Briefly, each fuzzy expert system model works through a three-step procedure including fuzzification, inference engine and defuzzification as exhibited in **Fig. 1**.

2. Experimental

2.1. Materials

Raw fly ash was collected from a combustion test furnace in Alborz-e-sharghi Coal Company located in Shahrood (Iran) with detailed chemical composition listed in **Table 1**. It was verified that the fly ash was environmentally-friendly with commercial utilization in traditional areas including concrete, pavement and dam. The standard solution of Cr (VI) was prepared by dissolving $K_2Cr_2O_7$ (Merck) into 1000 mL of distilled water in a 1 L volumetric flask. It was further diluted to predetermined volumes and concentrations with distilled water depending on experimental conditions. All the chemical reagents used in this study were of analytical grade, purchased from Merck. HCl (1 M, 0.1 M), HNO_3, (1 M, 0.1 M) and NaOH (1 M, 0.1 M) solutions were used for pH adjustment.

2.2. Adsorbent synthesis

According to the research investigated by Sharma et al. [7], washing samples with hot water could remove some alkali and alkaline earth elements such as K_2O, Na_2O, CaO and MgO from raw ash; therefore, the consumption of hydrochloric acid in the process of sorbent synthesis would be reduced. FA3 was prepared according to the following procedure: initially, 3 g of raw fly ash was added into 250 mL of water and the mixture was stirred and heated up to 95 $^{\circ}$C for 1 h. The insoluble part of the mixture was filtrated and rinsed repeatedly until the pH of leachate remained constant at approximate value of 6-7, and then the insoluble material was dried at 100 $^{\circ}$C for 2 h. Afterwards, 100 mL of 1 M HCl solution was added to the pretreated fly ash and the mixture was sonicated for 2 h and placed steadily at 60 $^{\circ}$C for 30 min after which the transparent solution gradually became yellow. 1 M NaOH solution was added dropwise into the above solution until the final pH reached the approximate value of 6, and an orange gel appeared. This step was followed by continuous vibration of the mixture for 1 h, and aging at 75 $^{\circ}$C for 3 days. Finally, the slurry was centrifuged and continuously rinsed several times with distilled water

until the pH of the leachate remained constant, then dried at 75 °C for 24 h. After drying, it was powdered and then kept in a polyethylene bottle.

In order to examine the properties of the acidic product obtained after acid treatment of raw fly ash at 60 °C for 30 min using HCl solution, it was centrifuged to separate the insoluble materials from the mixture, washed three times with distilled water and then dried at 75 °C for 24 h. The final product was identified as acidified fly ash (FA2).

2.3. Analysis

X-ray diffraction (XRD) analysis of FA1, FA2 and FA3 was performed by X-ray diffractometer (GBC made, Australia) using Cu Kα radioactive source in the range of 10° to 60° with operating conditions of 35 kV and 28.5 mA. JCPDS (Joint Committee on Powder Diffraction Standards) files were used to identify the crystalline compounds. Morphologies of FA1, FA2 and FA3 were monitored using field emission scanning electron microscopy (FE-SEM, HITACHI, S-4160, Japan).

The presence of functional groups on FA1, FA2 and FA3 was investigated using Fourier transform infrared spectroscopy (FT-IR, ECTOR-UKER, Germany) in wavenumber range of 4000–400 cm^{-1}.

Particle size distribution of the three samples was obtained using laser particle size (LPS) technology on a laser particle sizer (Master size 2000, Malvern Co, UK).

Brunauer-Emmet-Teller (BET) surface area was determined by fitting the linear portion of the N_2 sorption–desorption plot to BET equation. Moreover, pore size distribution was calculated based on Barrett-Joyner-Halenda (BJH) method (Micrometrics ASAP 2000, USA) and Skeleton density and porosity of FA2 and FA3 were measured based on water displacement method. Porosity was calculated using the following equation [10].

$$\varepsilon_p = 1 - \frac{\rho_s}{\rho_p} \quad (1)$$

where, ε_p is the porosity, ρ_s is the skeleton density (g/cm), and ρ_p is the density of the sorbent (g/cm). After sorption experiments, the supernatants were collected and concentration of Cr (VI) was measured by an atomic absorption spectrophotometer (GBC 302, Australia).

2.4. Batch sorption experiments

The effect of experimental conditions was studied in order to achieve the maximum Cr (VI) removal. To optimize the sorption process, different parameters including pH, contact time, initial Cr (VI) concentration and sorbent dosage were considered. The solution pH was adjusted by HNO_3 and NaOH and the experiments were performed at ±25 $^{\circ}$C. In each experiment, a desired amount of the sorbent was added into the samples, and the mixture was shaken at 250 rpm. After the predetermined time, the sorbent was filtered and Cr (VI) concentration in the supernatant was determined. All experiments were carried out twice and the mean values of concentrations were reported with the experimental error < 4 %. The removal efficiency (%) of Cr (VI) was calculated using the following equation [27]:

$$Removal\ efficiency(\%) = \frac{C_i - C_f}{C_i} 100 \quad (2)$$

where, C_i and C_f are the initial and final concentration of Cr (VI) (mg/L), respectively.

The sorption capacity at time t, q_t (mg/g), was obtained as follows:

$$q_t = \frac{(C_i - C_t) \times V}{M} \quad (3)$$

where, C_i and C_t (mg/L) are the concentrations of Cr (VI) at initial and at given time t, respectively, V (L) is the volume of the solution and M (g) is the mass of FA3. The equilibrium sorption capacity, q_e (mg/g), can be calculated using the following equation:

$$q_e = \frac{(C_i - C_e) \times V}{M} \quad (4)$$

where, C_e is the Cr (VI) concentration at equilibrium (mg/L).

3. Results and discussion

3.1. Characterization of the products

Fig. 2 illustrates the X-ray diffraction (XRD) patterns of FA1, FA2, and FA3 in which the main diffraction peaks of FA1 are assigned to quartz (SiO_2), hematite (Fe_2O_3), anhydrite ($CaSO_4$), magnetite (Fe_3O_4) and lime (CaO).

In **Table 1**, in spite of the fact that the aluminum mineralogical phase such as mullite cannot be observed in the sample, the content of Al_2O_3 is approximately 28.73 % which differs from the results reported before.

In FA1 XRD pattern, quartz is denoted as the main crystalline phase along with minor contents of hematite, magnetite and anhydrite, indicating that the content of quartz increases while the contents of Fe containing minerals (hematite and magnetite) decrease after acidic treatment [28]. As can be seen in FA3 XRD pattern, no new diffraction peaks appear and no new crystalline phase is formed in comparison to FA2. The peaks of magnetite and anhydrite disappeared and the peak intensity of quartz increased, confirming that the structure of the material is changed and new substance loaded on the surface of final product is amorphous. [29].

The FT-IR spectra of FA1, FA2 and FA3 are illustrated in **Fig. 3**. The band located at 1135 cm^{-1} is assigned to the vibration of Fe–O bond and the band at 1033 cm^{-1} is attributed to the asymmetric stretching vibration of T–O (T=Si, Al) [30]. Comparison of peaks indicates that a great portion of iron oxide and aluminum oxide was dissolved in HCl solution; however, the typical bands of quartz became more obvious, which could be attributed to quartz inertness and enrichment in FA2 [28]. The new bands observed at 3573 and 3379 cm^{-1} in the spectra of FA3

and FA2 are assigned to O–H stretching vibration and deformation of O–H vibration bond, respectively, implying that the new substance is in the form of hydroxyl compound [31]. According to FT-IR spectra of FA1, FA2 and FA3, the strong broad bands located at 3511, 3573 and 3376 cm^{-1} indicate the presence of hydroxyl groups on the fly ash [32,33].

The sharp peaks observed at 1033, 912 and 1016 cm^{-1} in FA1, FA2 and FA3 are due to the presence of Al atoms in the tetrahedral sites of silica frame work [34]. The bands at 734 and 622 cm^{-1} in FA1, 574 cm^{-1} in FA2 and 576 cm^{-1} in FA3 are attributed to the quartz in fly ash [35]. The bands between 800 and 500 cm^{-1} are associated to the tetrahedral vibrations of the secondary building units (SBU) and fragments of alumina silicate structure. These bands are commonly related to the single or double rings (depending on the structure of the material) or TO_4 (T= Si, Al) tetrahedral bonds [36].

The changes in the morphology of FA1, FA2, and FA3 are shown in **Fig. 4a**, **Fig. 4b** and **Fig. 4c**, respectively, with FA3 powder being drastically different from the original ash. The surface of FA3 is entirely covered by hydroxyl groups and gets into porous network structure, while the size of granule increases sharply.

From LPS analysis, the mean particle sizes of FA1 and FA3 were calculated to be 4.18 and 22.18 μm, respectively. The final product is nearly 5 times larger than FA1, which can efficiently enhance the adsorptive properties in the separation process. The pore size distribution analysis showed that the pore size of FA3 was in the range of 18 Å to 640 Å with average size of 38 Å and porosity of 23.6 %.

3.2. Loading mechanisms

Fly ash is rich in aluminum and iron oxides, and is thought to be a very important source of pre-mined material. Hence, many researchers have studied the ash leachability under acidic

conditions for the extraction of alumina, iron and other heavy metal elements. When fly ash contacts with hydrochloric acid, most of the metals such as Fe and Al can leach into the solution through the following reactions [10]:

$$Fe_2O_3 + 6\ H^+ \rightarrow Fe^{+3} + 3\ H_2O \quad (5)$$

$$Fe_3O_4 + 8\ H^+ \rightarrow Fe^{+2} + 2\ Fe^{+3} + 4\ H_2O \quad (6)$$

$$Al_2O_3 + 6\ H^+ \rightarrow 2\ Al^{+3} + 3\ H_2O \quad (7)$$

During the reaction, the color of the mixture in the conical flask gradually changed to light yellow due to the dissolution of Fe^{+3} in the fly ash. When the slurry was adjusted with sodium hydroxide solution to raise its alkalinity, a slurry containing Fe^{+2}, Fe^{+3} and Al^{+3} formed according to the following reactions. The slurry of mixture changed color from light yellow to orange, indicating that Fe ion precipitated from the solution.

$$Fe^{+2} + 2oH^- \rightarrow Fe(oH)_2 \downarrow \quad (8)$$

$$4Fe(oH)_2 + o_2 + 2H_2o \rightarrow 4FeooH \downarrow +4H_2o \quad (9)$$

$$Fe^{+3} + 3oH^- \rightarrow FeooH \downarrow +4H_2o \quad (10)$$

$$Al^{+3} + 3oH^- \rightarrow Al(oH)_3 \downarrow \quad (11)$$

By adjusting solution pH to 3.0 and 3.5, Fe and Al ions precipitate in aqueous media. In this research, the precipitation of Fe $(OH)_2$ was firstly observed in the solution; since the solution color changed from white to orange, indicating the oxidation of Fe $(OH)_2$ to Fe $(OH)_3$. When fly ash contacts with the acidic solution, the Si–O bonds on the surface of spherical glassy particles increase due to the dissolution of other metal elements [10,27-29]. On the other hand, when FeOOH is precipitated and coated on the surface of the residual fly ash, Fe–Si surface complex (typically, Fe–O–$Si(OH)_3$) forms between Fe and Si which ultimately increases the physical strength of the sorbent. This was confirmed through Cr (VI) batch sorption experiments, where

no disintegration of the sorbent happened after treatment. During the filtration experiment, it was also revealed that FA3 sorbent was easily filtered with a filter paper (Grade 42, Whatman), with particle retention size of 25 μm. In contrast, a significant portion of particles passed through the similar filter paper during the filtration of a laboratory-made pure FeOOH suspension. This observation indicated that no FeOOH suspension was disintegrated from the sorbent [10]. Furthermore, the silica on the surface of the particle could block or retard the transformation of the initially formed FeOOH to crystalline iron oxides such as ferrihydrite, goethite and hematite [10]. Cr (VI) sorption with the crystalline form of FeOOH, e.g. goethite and ferrihydrite is not desired; thus, it has much less surface area than its amorphous form and reduces the Cr (VI) removal capability of FA3. In brief, high Cr (VI) removal efficiency of FA3 and its high physical strength were attained in this system during the process.

3.3. Effect of pH

The effect of solution pH on Cr (VI) sorption by FA3 was studied at different pH values in the range of 1.5 to 13. As it is demonstrated in **Fig. 5**, Cr (VI) is removed effectively in the initial pH range of 1.5 to 8. The highest amount of Cr (VI) sorption is achieved at pH=6, with sorption capacity of 21.22 mg/g; therefore, FA3 can be considered as an effective sorbent over a wide range of pH in comparison to other sorbents prepared by the addition of extra iron source. This wide range of pH can be attributed to the existence of aluminum hydroxide on the surface of the sorbent. Accordingly, the removal mechanisms of FA3 for Cr (VI) sorption include not only sorption but also interactions with both iron and aluminum oxides on the surface of FA3 [29].

In order to compare the removal efficiency of FA3 for Cr (VI) adsorption by means of raw fly ash, an experiment was performed at pH=6 under the same experimental conditions. The

sorption capacities obtained by raw ash and FA3 for Cr (VI) sorption were 10.13 and 21.22 mg/g, respectively, indicating that FA3 was 2 times more effective than raw ash at the same experimental conditions. This phenomenon could be mainly attributed to the porous structure of FA3 and its high specific surface area in comparison to FA1 (the BET values of FA1 and FA3 was 8.22 and 154.12 m^2/g, respectively). In this regard, the introduction of hydroxyl groups on the surface of the raw ash increased the specific surface area nearly 18 times; consequently, enhanced the sorption efficiency.

3.4. Effect of contact time

In order to obtain the sorption equilibrium time, Cr (VI) sorption experiments were conducted in which FA3 dose and initial Cr (VI) concentration were 2 g/L and 53 mg/L, respectively. **Fig. 6** indicates that a sharp increase occurs in the first 6 h of sorption and the equilibrium state is achieved after 8 h.

3.5. Effect of sorbent dose

The effect of sorbent dose on Cr (VI) sorption is illustrated in **Fig .7**. It is observed that Cr (VI) removal efficiency sharply increases when adsorbent dose is increased. Cr (VI) sorption rises slowly by the addition of more sorbent, until it is fully adsorbed.

3.3.4. Effect of Cr (VI) initial concentration

2 g/L of sorbent was added into Cr (VI) solutions at pH=6 with various initial concentrations in the range of 1 to 100 mg/L. The effect of different Cr (VI) concentrations on the removal efficiency is illustrated in **Fig. 8**. It is observed that Cr (VI) removal efficiency decreases by increasing its initial concentration, indicating that Cr (VI) sorption on FA3 is dependent on the availability of binding sites; for instance, when initial Cr (VI) concentration is

1 mg/L, its removal efficiency is above 99 % and the final concentration decreases to below 0.01 mg/L.

3.6. Sorption kinetics

Various kinetic models including Morris–Weber intra-particle diffusion, Lagergren pseudo-first-order, and pseudo-second-order were used to verify the validity of experimental data regarding Cr (VI) sorption on FA3. Sorption kinetics describe the solute uptake rate of a system, which controls the residence time of adsorbate uptake at solid-solution interface including the diffusion process. It is assumed that there is no mass transfer resistance (both external and internal) in the overall sorption process; therefore, residual metal ion concentration in the solution can be used to study the sorption kinetics.

3.6.1. Morris–Weber model

Morris–Weber was applied to the data obtained from Cr (VI) sorption onto FA3 in order to investigate the concentration change of Cr (VI) in the solution [37]:

$$q_t = K_{id}(t)^{0.5} + C \quad (12)$$

In **Table 2**, the correlation coefficient is 0.89 and the rate constant, K_{id}, calculated from the slope of the linear plot is 7.679 1/h.

Internal-particle diffusion may involve pore and/or surface diffusion. Its plot indicates multi-linearity in the process indicating three operational steps. The first stage with high slope can be attributed to the diffusion of adsorbate through the external surface of the sorbent or the boundary surface diffusion of sorbate molecules, while the second stage describes the gradual sorption, where intra-particle diffusion is rate-limiting. The third stage is the final equilibrium due to the reduction of sorbate concentration in the solution and also the interior active sites of

sorbent. The three stages in the plot suggest that the sorption process occurs through surface sorption and intra-particle diffusion.

3.6.2. Pseudo-first-order model

In 1898, Lagergren presented a pseudo-first-order equation for sorption of liquid/solid systems based on solid capacity. In this equation, the change in the rate of sorption uptake with time is directly proportional to the difference in saturation concentration and the amount of solid uptake. Lagergren model is the most widely used rate equation in sorption processes which is expressed by the following equation [38]:

$$\log(q_e - q_t) = \log q_e - \left(\frac{K}{2.303}\right)t \quad (13)$$

where, q_e is the sorption capacity at equilibrium and K is the pseudo-first-order rate constant. The applicability of the model for Cr (VI) sorption onto FA3 was investigated by plotting log ($q_e - q_t$) versus time 't'. The correlation coefficient and rate constant calculated from the slope of the linear plot were 0.985 and -0.244 1/h, respectively.

3.6.3. Pseudo-second-order model

Pseudo-second-order model was applied to fit the data obtained from Cr (VI) sorption onto FA3 by the following equation [39, 40]:

$$\frac{t}{q_t} = \frac{1}{k_2 q_e^2} + \frac{t}{q_e} \quad (14)$$

The rate constant and correlation coefficient from linear plot of t/q_t versus t were found to be 9.15×10^{-3} 1/h and 0.97, respectively.

The results revealed that the sorption process was controlled by pseudo-first-order equation. The basic assumption of pseudo-second-order model suggests that the rate-limiting step in sorption process might be due to the chemisorption involving valence forces through

sharing or exchanging electrons between sorbent and sorbate [41,42]. The statistical results and kinetic constants are given in **Table 2**.

3.7. Adsorption isotherm models

Isotherm models are the mathematical representation of the relationship between metal concentration in solution and the amount of metal adsorbed onto the equivalent sorption sites at a constant temperature [43].

3.7.1. Langmuir model

Langmuir model is valid for monolayer sorption onto surfaces containing finite number of identical sorption sites. It is presented by the following equation [44,45]:

$$q_e = \frac{k_l q_{\max} c_e}{1 + k_l c_e} \quad (15)$$

where, q_m is the maximum sorption capacity of sorbent for the metal ion (mg/g). The linear form of Eq. (15) is commonly used to determine q_m and K_L values from the plot of C_e/q_e versus C_e [46, 47].

$$\frac{C_e}{q_e} = \frac{1}{q_o K_L} + \frac{C_e}{q_o} \quad (16)$$

3.7.2. Freundlich model

While Langmuir isotherm assumes that the enthalpy of sorption is independent of the amount of metal adsorbed, Freundlich model basically assumes that sorption is done on heterogeneous surfaces with a logarithmic decrease in sorption enthalpy, when the fraction of occupied sites increases. It is given as follows [48, 49]:

$$q_e = k_F \left(C_e\right)^{\frac{1}{n}} \quad (17)$$

where K_F and (1/n) are the Freundlich constant and sorption intensity, respectively. Freundlich equation is generally linearized in logarithmic form to determine the constants as follows [50]:

$$\log(q_e) = \log(k_F) + \frac{1}{n}\log(C_e) \quad (18)$$

Equilibrium constants are evaluated from the intercept and slope of the linear plot of log q_e versus log C_e.

3.7.3 Dubinin–Radushkevich isotherm

In order to determine the physical or chemical nature of sorption, Dubinin–Radushkevich (D–R) model is commonly used by the following linearized form [51]:

$$Ln(q_e) = Ln(q_m) - \beta\varepsilon^2 \quad (19)$$

where, β is the activity coefficient related to the mean sorption energy and ε is the Polanyi potential with the following equation:

$$\varepsilon = RTLn\left[\left(1 + \frac{1}{C_e}\right)\right] \quad (20)$$

The values of β and q_m can be determined from the slope and intercept of the linear plot of ln q_e versus ε^2. The statistical results along with isotherm constants are given in **Table 3** from which it can be concluded that Cr (VI) sorption by FA3 is well fitted using Freundlich, Langmuir and D–R models with considerable correlation coefficients. By comparing the correlation coefficients, it is clear that Freundlich model fits the experimental data better than the other two isotherm models. Although Freundlich model predicts the exponential distribution of active sites with their energies and provides information about the surface heterogeneity, it does not predict any saturation point for sorption sites by sorbate; thus, infinite surface coverage can be predicted mathematically. In contrast, D–R isotherm relates the heterogeneity of energies close to the sorbent surface [42,51].

3.8. Effect of temperature on Cr (VI) sorption and thermodynamic parameters

Since most effluents containing heavy metals are produced at high temperature, temperature is an important factor in the real applications of sorption process. It has two main effects on sorption process. Increasing temperature enhances the sorbate diffusion rate across the external boundary layer and the internal pores of sorbent due to a decrease in the viscosity of solution. In addition, for a specific sorbate, temperature is directly proportional to the equilibrium capacity of sorbent. To study the effect of temperature on Cr (VI) removal efficiency, the experiments were carried out using 25 mL of solutions with 53 mg/L initial Cr (VI) concentration at different temperatures ranging from 25 °C to 45 °C. The results in **Table 4** show that the removal efficiency increases when temperature is increased, revealing the endothermic nature of the sorption process.

In any sorption system, the values of thermodynamic parameters are important for practical applications. The spontaneity of sorption process can be specified by evaluating both energy and entropy. In this regard, the equilibrium sorption capacity of 53 mg/L initial Cr (VI) concentration at different temperatures from 25 °C to 45 °C was examined to obtain the thermodynamic parameters by the following equation [52]:

$$K_c = \frac{F_e}{1-F_e} \quad (21)$$

$$lnK_C = \left(\frac{\Delta S}{R}\right) - \left(\frac{\Delta H}{RT}\right) \quad (22)$$

$$\Delta G = -RTlnK_C \quad (23)$$

where, K_C, ΔH, ΔS, ΔG, R and T are thermodynamic equilibrium constant, enthalpy change (J/mol), entropy change (J/mol), Gibbs free energy, universal gas constant (8.314 J/mol K), and temperature (K), respectively. **Fig. 9** shows a linear relationship between ln K_C versus 1/T. The thermodynamic parameters of Cr (VI) sorption onto FA3 at various temperatures are summarized in **Table 5**. The enthalpy change (ΔH) is positive, indicating that Cr (VI) sorption onto FA3 is

endothermic and increases at higher temperatures. The positive value of ΔS indicates the increasing randomness at solid-liquid interface during the sorption process. The negative values of ΔG and decrease in its values at higher temperatures indicate the feasibility and spontaneity of Cr (VI) sorption onto FA3.

3.9. Cr (VI) desorption from the sorbent

Regeneration of sorbent is considered as a main factor in its industrial applications for treatment of wastewater. In this study, desorption of Cr (VI) from FA3 was performed using a batch system in which the ability of NaOH to desorb Cr (VI) was investigated. The sorbent loaded with initial concentration of 53 mg/L of Cr (VI) was placed in the desorption medium containing 25 mL of 0.2 M NaOH and finally the amount of desorbed Cr(VI) was measured after 8 h. **Table 6** clearly demonstrates that FA3 can be repeatedly used without significant reduction in the sorption capacity toward Cr (VI). The ability of 0.2 M NaOH to desorb Cr (VI) ions may be attributed to its ion exchange ability. It can be suggested that the high concentration of OH ions at high pH via ion exchange mechanism is the reason for the replacement of the adsorbed ions. After three consecutive cycles of adsorption-desorption, the uptake capacity of FA3 decreased because the binding sites on the surface of the sorbent are destroyed or morphologically changed.

3.10. Cost of sorbent production

The cost of the precursor or the adsorbent depends on various factors including the availability of initial waste material, the processing required, the treatment conditions and both recycle and lifetime issues. Since raw fly ash is available at the power plant, hence, there are only transportation, laying and rolling costs. The production costs of various sorbents based on fly ash are rarely reported in the literatures; for example, the waste bagasse fly ash price was

reported 0.002 US$ per kg, and with considering the transportation cost, chemicals, electrical energy, etc., used in the process, the final product would cost approximately 0.009 US$ per kg. Investigations on different fly ash sorbents illustrated that the cost of materials was ≤ 0.3 US$ per kg making them useful sorbents in terms of cost in comparison with commercial activated carbons which normally cost more than 3 US$ per kg. The expected outcomes of the sorbent production would be economical given any increase in the costs of synthesis process. According to the primary assessments, in the worst conditions, the product would have at least four times interest per Kg. As mentioned before, the sorbent studied in this work is eco-friendly, reusable and cost-effective in comparison with other commercialized products.

3.11. Fuzzy modeling for Cr (VI) sorption prediction

Fuzzy logic modeling applied in this study had four input variables including pH, contact time, adsorbent dose, and Cr (VI) concentration whose ranges were [1,13], [1,10], [0,10] and [0,100] respectively. The designed fuzzy inference system has an output named removal efficiency of Cr (VI) in the ranges of [0,100] as shown in **Fig. 10**. Multiple membership functions consisting of VVL, VL, L, M, H, VH and VVH were considered for input variables (pH, t, D, C). The names of these seven fuzzy sets were defined “very very low”, “very low”, “low”, “medium”, “high” “very high” and “very very high”. Several membership functions such as VVL, VL, L, M (1-8), H, VH (1-2), VVH (1-2) were used to call the output variables “very very low”, “very low”, “low”, “moderate”, “high”, “very high” and “very very high” (**Fig. 10**). In addition, all membership functions (MFs) used for both input and output variables were selected in triangle shapes. Therefore, the prevalent mathematical definition of triangular MFs is admissible for this modeling. It states that the triangular curve is a function of vector x that depends on three scalar parameters a, b and c as follows:

$$f(x,a,b,c) = \begin{cases} 0 & x \le a \\ & or \\ & x \ge c \\ \frac{x-a}{b-a} & a \le x \le b \\ \frac{c-x}{c-b} & b \le x \le c \end{cases} \quad (24)$$

The compact form of function (24) is represented as follows:

$$f(x,a,b,c) = \max(\min(\frac{x-a}{b-a}, \frac{c-x}{c-b}), 0) \quad (25)$$

Parameter ‘b’ is located at the peak of triangle while ‘a’ and ‘c’ are at its both sides named triangle feet [53]. Practically, local inferences play significant role in modeling a fuzzy inference system. In other words, each rule is initially inferred and thereafter the results of individual rules inferences would be gathered. There are several inference methods in fuzzy systems including the max-min, the max-product and the sum-product methods. In these methods, max or sum are indicative of the aggregation factor while min or prod are indicative of the fuzzy implication operator. From relevant literatures, the best method to calculate the fuzzy relations is the max-min method which computationally presents a good and expressive setting for constraint propagation [25,54]. In the defuzzification step, the results of fuzzy are defuzzified to obtain an obvious output. Maximum matching and centroid defuzzification are the most famous defuzzification methods usually used in this step. In the present study, the max-min aggregation and centroid defuzzification methods are used to design the fuzzy rules. Moreover, the aggregation operation of fuzzy sets of input variables is conducted and ultimately the fuzzy reasoning results of outputs are obtained. The schematic of the fuzzy inference system for Cr (VI) removal efficiency is shown in **Fig. 11**.

The relationship between the input variables including pH, contact time, adsorbent dose, and initial concentration of Cr (VI) versus the removal efficiency as output is formed by fuzzy model rules. In fact, the expectations from adsorption process were considered in the form

of fuzzy rules and three-dimensional surfaces are shown in **Fig. 12**. The removal efficiency of Cr (VI) as a response was calculated for each input variable using fuzzy modeling in Matlab software. **Fig. 13** clearly demonstrates that the predicted data obtained from dynamic simulation have a little deviation from the experimental data. In fact, fuzzy inference system presents an acceptable performance in the prediction of removal efficiency with good agreement between the predicted and experimental data. The correlation coefficient (R^2) is greater than 0.95 by the liner regression as shown in **Fig. 14**. Also, several important parameters including average relative error (ARE), absolute average relative error (AARE) and standard deviation (SD) were calculated in order to measure the accuracy of the predicted data obtained by fuzzy model. **Table 7** exhibits the computation results of ARE, AARE and SD obtained from the proposed fuzzy model which approve its considerable ability in the prediction of Cr (VI) removal efficiency. The values of ARE, AARE and SD are computed by the following equations:

$$ARE = \frac{1}{N}\sum_{i=1}^{N}\left(\frac{X_{experimental(i)}-X_{calculated(i)}}{X_{experimental(i)}}\right) \quad (26)$$

$$AARE = \frac{1}{N}\sum_{i=1}^{N}\left(\left|\frac{X_{experimental(i)}-X_{calculated(i)}}{X_{experimental(i)}}\right|\right) \quad (27)$$

$$SD = \sqrt{\frac{1}{N-1}\sum_{i=1}^{n}\left(\left|\frac{X_{experimental(i)}-X_{calculated(i)}}{X_{experimental(i)}}\right| - AARE\right)^2} \quad (28)$$

The performance of fuzzy logic model applied in the present study was compared with other usable models in the prediction of removal efficiency. **Table 8** represents the experimental and statistical results reported in the literatures, confirming that the developed statistical model used in the present work reasonably demonstrates precise predictions in comparison with

experimental observations. In addition, a sensitivity analysis was employed to find the effect of each input parameter on output variable in fuzzy model (**Fig. 15**). To produce the sensitivity response for each parameter, one of the input variables was varied at identical intervals and the other variables were kept unchanged. The results show that although all parameters have remarkable effects on the output variable, solution pH was found to be the most effective parameter in Cr (VI) removal efficiency among others. In summary, fuzzy logic model was highly effective to find complex non-linear relationships available in the sorption process.

4. Conclusions

In this research, hydrous iron oxide/aluminum hydroxide composite loaded on coal fly ash (FA3) was synthesized as a potential sorbent for Cr (VI) sorption. XRF. XRD, FT-IR, SEM, LPS and BET surface area were used to characterize the sorbent. The FA3 mean particle sizes were 5 times greater than the original fly ash, thus, it could be easily separated from the aqueous solution after Cr (VI) sorption. Moreover, the sorbent had porous structure with specific surface area of 154 m^2/g that was 18 times greater than the original fly ash. The maximum removal percentage of Cr(VI) was 84.9 % with a maximum sorption capacity of 33.3 mg/g at optimum conditions of pH=6, 2 g/L adsorbent dose, 8 h contact time and 53 mg/L initial Cr (VI) concentration. According to the correlation coefficient (R^2) values obtained from the sorption kinetic and isotherm models, it can be mentioned that the sorption process was controlled by pseudo-first-order model and equilibrium data were fitted well to Freundlich model. Thermodynamic results revealed that the sorption was endothermic, feasible and spontaneous. Cr (VI) desorption from FA3 was investigated using 0.2 M NaOH. The maximum desorption efficiency was 81 % that clearly confirmed the appropriate performance of FA3. Furthermore, based on experimental data, the fuzzy logic model was applied to predict the removal

performance of the sorbent. The Mamdani model of fuzzy interface system was developed by using 24 If-Then rules based on triangular membership functions for both input variables and output. Removal efficiency of Cr (VI) was successfully predicted by the proposed fuzzy logic model. The correlation coefficient, average relative error (ARE), absolute average relative error (AARE) and standard deviation (SD) were 0.95, 1.36, 6.48 and 9.68, respectively. In order to reach the real and precise prediction of Cr (VI) removal efficiency by fuzzy logic model, additional input and output variables can be evaluated considering the effects of unexpected input alterations on outputs. Meanwhile, various types of membership functions or their combinations can be used to enhance the prediction performance of the proposed diagnosis system based on fuzzy logic model.

References

[1] C. Paduraru, L. Tofan, Investigations on the possibility of natural hemp fibers use for Zn (II) ions removal from wastewaters, Environ. Eng. Manag. J, 7 (2008) 687-693.

[2] T. Khan, V. Singh, I. Ali, Sorption of Cd (II), Pb (II) and Cr (VI) metal ions from wastewater using bottom fly ash as low cost sorbent, J. Environmen. Protect. Sci, 3 (2009) 124-132.

[3] S.R.M. Rao, V.V.B. Rao, Removal of Hexavalent Chromium from electroplating industrial effluents by using hydrothermally treated fly ash, J. Appl. Sci, 7 (2007) 2088-2092.

[4] D. Wu, Y. Sui, S. He, X. Wang, C. Li, H. Kong, Removal of trivalent chromium from aqueous solution by zeolite synthesized from coal fly ash, J. Hazard. Mater, 155 (2008) 415-423.

[5] R.M. Hlihor, M. Gavrilescu, Removal of some environmentally relevant heavy metals using low-cost natural sorbents, Environ. Eng. Manag. J, 8 (2009) 353-372.

[6] Q. Chen, Z. Luo, C. Hills, G. Xue, M. Tyrer, Precipitation of heavy metals from wastewater using simulated flue gas: Sequent additions of fly ash, lime and carbon dioxide, Water Res, 43 (2009) 2605-2614.

[7] Y. Sharma, V. Srivastava, J. Srivastava, M. Mahto, Reclamation of Cr (VI) rich water and wastewater by wollastonite, Chem. Eng. J, 127 (2007) 151-156.

[8] S. Andini, R. Cioffi, F. Colangelo, F. Montagnaro, L. Santoro, Adsorption of chlorophenol, chloroaniline and methylene blue on fuel oil fly ash, J. Hazard. Mater, 157 (2008) 599-604.

[9] S. Coruh, O.N. Ergun, Use of fly ash, phosphogypsum and red mud as a liner material for the disposal of hazardous zinc leach residue waste, J. Hazard. Mater, 173 (2010) 468-473.

[10] Y. Li, F.S. Zhang, F.R. Xiu, Arsenic (V) removal from aqueous system using adsorbent developed from a high iron-containing fly ash, Sci. Total. Environ, 407 (2009) 5780-5786.

[11] E. Murnleitner, T.M. Becker and A. Delgado, State detection and control of overloads in the anaerobic wastewater treatment using fuzzy logic, Water Research, 36(1) (2002) 201–211.

[12] H. Mingzhi, Y. Ma, W. Jinquan, W. Yan, Simulation of a paper mill wastewater treatment using a fuzzy neural network, Expert Systems with Applications 36(3) Part 1 (2009) 5064-5070.

[13] M.A. Akcayol, Application of adaptive neuro-fuzzy controller for SRM, Adv. Eng. Software, 35 (2004) 129–137.

[14] G. Feng, A survey on analysis and design of model-based fuzzy control systems, Fuzzy Systems, IEEE Transactions on 14(5) (2006) 676 – 697, ISSN: 1063-6706.

[15] J. I. Horiuchi, M. Kamasawa, H. Miyakawa and M. Kishimoto, Phase control of fed-batch culture for α-amylase production based on culture phase identification using fuzzy inference, Journal of Fermentation and Bioengineering 76(3) (1993) 207-212.

[16] L.A. Zadeh, Fuzzy sets, Inf. Control 8 (1965) 338–353.

[17] R. Sadiq, M.A. Al-Zahrani, A.K. Sheikh, T. Husain, Sh. Farooq, Performance evaluation of slow sand filters using fuzzy rule-based modeling, Environ. Model. Software 19 (2004) 507–515.

[18] T. Takagi, M. Sugeno, Fuzzy identification of systems and its application to modelling and control, IEEE Trans. Syst. Man Cybern. Part B Cybern. 15 (1985) 116–132.

[19] E.H. Mamdani, S. Assilian, An experiment in linguistic synthesis with a fuzzy logic controller, Int. J. Man Mach. Stud. 7 (1975) 1–13.

[20] Z. Huang, J. Hahn, Fuzzy modeling of signal transduction networks, Chem. Eng. Sci. 64 (2009) 2044–2056.

[21] L.A. Zadeh, Making computer think like people, IEEE Spectr. 8 (1984) 26–32.

[22] S. Haack, Do we need fuzzy logic? Int. J. Man-Mach. Stud. 11 (1979) 437–445.

[23] A. Altunkaynak, S. Chellam, Prediction of specific permeate flux during cross flow microfiltration of polydispersed colloidal suspensions by fuzzy logic models, Desalination 253 (2010) 188–194.

[24] M. Alvarez Grimaa, R. BabusIka, Fuzzy model for the prediction of unconfined compressive strength of rock samples, Int. J. Rock Mech. Min. Sci. 36 (1999) 339–349.

[25] R. Babuska, Fuzzy Modeling for Control, Kluwer Academic Publishers, Massachusetts, 1998.

[26] D.R. Keshwani, D.D. Jones, G.E. Meyer, R.M. Brand, Rule-based Mamdani-type fuzzy modeling of skin permeability, Appl. Soft Comput. 8 (2008) 285–294.

[27] M.H. Isa, N. Ibrahim, H.A. Aziz, M.N. Adlan, N.H.M. Sabiani, A.A.L. Zinatizadeh, S.R.M. Kutty, Removal of chromium (VI) from aqueous solution using treated oil palm fiber, J. Hazard. Mater, 152 (2008) 662-668.

[28] S. Khaitan, D.A. Dzombak, G.V. Lowry, Neutralization of bauxite residue with acidic fly ash, Environ. Eng. Sci, 26 (2009) 431-440.

[29] S. Lu, S. Bai, L. Zhu, H. Shan, Removal mechanism of phosphate from aqueous solution by fly ash, J. Hazard. Mater, 161 (2009) 95-101.

[30] J. Ayala, F. Blanco, P. Garcia, P. Rodriguez, J. Sancho, Asturian fly ash as a heavy metals removal material, Fuel, 77 (1998) 1147-1154.

[31] G. Atun, G. Hisarli, A.E. Kurtoglu, N. Ayar, A comparison of basic dye adsorption onto zeolitic materials synthesized from fly ash, J. Hazard. Mater, 187 (2011) 562–573.

[32] Y.F. Yang, G.S. Gai, Z.F. Cai, Q.R. Chen, Surface modification of purified fly ash and application in polymer, J. Hazard. Mater, 133 (2006) 276-282.

[33] E. Álvarez, X. Querol, F. Plana, A. Alastuey, N. Moreno, M. Izquierdo, O. Font, T. Moreno, S. Diez, E. Vázquez, M. Barra, Environmental, physical and structural characterisation of geopolymer matrixes synthesised from coal (co-) combustion fly ashes, J. Hazard. Mater, 154 (2008) 175-183.

[34] K. Hui, C. Chao, Synthesis of MCM-41 from coal fly ash by a green approach: Influence of synthesis pH, J. Hazard. Mater, 137 (2006) 1135-1148.

[35] S. Mohan, R. Gandhimathi, Removal of heavy metal ions from municipal solid waste leachate using coal fly ash as an adsorbent, J. Hazard. Mater, 169 (2009) 351-359.

[36] F. Škvára, L. Kopecký, V. Smilauer, Z. Bittnar, Material and structural characterization of alkali activated low-calcium brown coal fly ash, J. Hazard. Mater, 168 (2009) 711-720.

[37] H. Javadian, P. Vahedian, M. Toosi, Adsorption characteristics of Ni(II) from aqueous solution and industrial wastewater onto Polyaniline/HMS nanocomposite powder, Appl. Surf. Sci, 284 (2013) 13-22.

[38] P. Janos, J. Sypecka, P. Mlckovska, P. Kuran, V. Pilarova, Removal of metal ions from aqueous solutions by sorption onto untreated low-rank coal (oxihumolite), Sep. Purif. Technol, 53 (2007) 322-329.

[39] H. Javadian, Application of kinetic, isotherm and thermodynamic models for the adsorption of Co(II) ions on polyaniline/polypyrrole copolymer nanofibers from aqueous solution, J. Ind. Eng. Chem, 20 (2014) 4233-4241.

[40] C. Smaranda, D. Bulgariu, M. Gavrilescu, Equilibrium and kinetic studies of acid dye sorption onto soils from iasi area, Environ. Eng. Manag. J, 9 (2010) 57-66.

[41] K. Hui, C. Chao, S. Kot, Removal of mixed heavy metal ions in wastewater by zeolite 4A and residual products from recycled coal fly ash, J. Hazard. Mater, 127 (2005) 89-101.

[42] R. Krishna Prasad, S. Srivastava, Electrochemical degradation of distillery spent wash using catalytic anode: Factorial design of experiments, Chem. Eng. J, 146 (2009) 22-29.

[43] A. Papandreou, C. Stournaras, D. Panias, Copper and cadmium adsorption on pellets made from fired coal fly ash, J. Hazard. Mater, 148 (2007) 538-547.

[44] S. Wang, Z. Zhu, Sonochemical treatment of fly ash for dye removal from wastewater, J. Hazard. Mater, 126 (2005) 91-95.

[45] N. Singh, Adsorption of herbicides on coal fly ash from aqueous solutions, J. Hazard. Mater, 168 (2009) 233-237.

[46] H. Ghassabzadeh, A. Mohadespour, M. Torab-Mostaedi, P. Zaheri, M.G. Maragheh, H. Taheri, Adsorption of Ag, Cu and Hg from aqueous solutions using expanded perlite, J. Hazard. Mater, 177 (2010) 950-955.

[47] D. Sun, X. Zhang, Y. Wu, X. Liu, Adsorption of anionic dyes from aqueous solution on fly ash, J. Hazard. Mater, 181 (2010) 335-342.

[48] C. Orha, F. Manea, C. Ratiu, G. Burtica, A. Iovi, Obtaining and characterization of romanian zeolite supporting silver ions, Environ. Eng. Manag. J, 6 (2007) 541-544.

[49] C. Wang, J. Li, X. Sun, L. Wang, Evaluation of zeolites synthesized from fly ash as potential adsorbents for wastewater containing heavy metals, J. Environ. Sci, 21 (2009) 127-136.

[50] H. Cho, D. Oh, K. Kim, A study on removal characteristics of heavy metals from aqueous solution by fly ash, J. Hazard. Mater, 127 (2005) 187-195.

[51] V.K. Jha, M. Nagae, M. Matsuda, M. Miyake, Zeolite formation from coal fly ash and heavy metal ion removal characteristics of thus-obtained Zeolite X in multi-metal systems, J. Environ. Manage, 90 (2009) 2507-2514.

[52] H. Javadian, M. Torabi Angaji, M. Naushad, Synthesis and characterization of polyaniline/γ-alumina nanocomposite: A comparative study for the adsorption of three different anionic dyes, J. Ind. Eng. Chem, 20 (2014) 3890-3900.

[53] S.N. Sivanandam, S. Sumathi, S.N. Deepa, Introduction to Fuzzy Logic using MATLAB, Springer Berlin, Heidelberg New York, 2007.

[54] K.K. Ahn, D.Q. Truong, Online tuning fuzzy PID controller using robust extended Kalman filter, J. Process. Control 19 (2009) 1011–1023.

[55] A. R. Esfahani, S. Hojati, A. Azimi, M. Farzadian, A. Khataee, Enhanced hexavalent chromium removal from aqueous solution using a sepiolite-stabilized zero-valent iron nanocomposite: Impact of operational parameters and artificial neural network modeling, J. Taiwan Inst. Chem. Eng. 49 (2015) 172-182.

[56] T. N. Singh, V.K. Singh, S. Sinha, Prediction of Cadmium Removal Using an Artificial Neural Network and a Neuro- Fuzzy Technique, Mine Water Environ. 25 (2006) 214-219.

[57] I. P. Kotti, G. K. Sylaios, V. A. Tsihrintzis, Fuzzy logic models for BOD removal prediction in free-water surface constructed wetlands, Ecol. Eng. 51 (2013) 66– 74.

[58] B. Rahmaniana, M. Pakizeha, M. Esfandyaria, F. Heshmatnezhada, A. Maskookib, Fuzzy modeling and simulation for lead removal using micellar-enhanced ultrafiltration (MEUF), J. Hazard. Mater. 192 (2011) 585– 592.

[59] S. Mandal, S. S. Mahapatra, M. K. Sahu, R. K. Patel, Artificial neural network modeling of As(III) removal from water by novel hybrid material, Process Saf. Environ. Prot. 93 (2015) 249-264.

[60] M. Shanmugaprakash, V. Sivakumar, Development of experimental design approach and ANN-based models for determination of Cr (VI) ions uptake rate from aqueous solution onto the solid biodiesel waste residue, Bioresour. Technol. 148 (2013) 550–559.

[61] S. Mandal, S. S. Mahapatra, R. K.Patel**,** Neuro fuzzy approach for arsenic(III) and chromium(VI) removal from water, J. Water Process Eng. 5 (2015) 58–75.

[62] M. S. Podder, C. B. Majumder, The use of artificial neural network for modelling of phycoremediation of toxic elements As(III) and As(V) from wastewater using Botryococcus braunii, Spectrochin. Acta, Part A, 155 (2016) 130–145.

[63] N. G. Turan, B. Mesci, O. Ozgonenelc, The use of artificial neural networks (ANN) for modeling of adsorption of Cu(II) from industrial leachate by pumice, Chem. Eng. J. 171 (2011) 1091– 1097.

[64] S. M. Hosseini Asl, M. Ahmadi, M. Ghiasvand, A. Tardast, R. Katal, Artificial neural network (ANN) approach for modeling of Cr (VI) adsorption from aqueous solution by zeolite prepared from raw fly ash (ZFA), J. Ind. Eng. Chem. 19 (2013) 1044‑1055.

Table 1. XRF analysis of the fly ash.

Properties	**LIO**	**SiO_2**	**Al_2O_3**	**Fe_2O_3**	**CaO**	**MgO**	**SO_3**	**K_2O**	**Na_2O**
Percentage (mass, %)	0.98	37.88	28.73	18.07	11.54	1.79	0.38	0.34	0.29

Table 2. Kinetic constants for Cr (VI) sorption.

Lagergren pseudo-first-order	**K (1/h)**	**q_e (mg/g)**	**R^2**
	-0.244	33.3	0.9851
Pseudo-second-order	**K (1/h)**	**q_e (mg/g)**	**R^2**
	9.15×10^{-3}	31.79	0.971
Morris-Weber	**K_{id} (1/h)**	----------	**R^2**
	7.679	----------	0.8991

Table 3. Isotherm constants for Cr (VI) sorption.

Langmuir	**K_l (1/h)**	**q_m (mg/g)**	**R^2**
	0.048	70.028	0.9575
Freundlich	**K (1/h)**	**n**	**R^2**
	3.981	1.402	0.98
D-R	**q_m (mg/g)**	**β**	**R^2**
	27.385	-2×10^{-6}	0.815

Table 4. Effect of temperature on Cr (VI) removal efficiency.

	Temperature (ºC)		
	25	35	45
Removal Efficiency (%)	85	89	94

Table 5. Thermodynamic parameters for Cr (VI) sorption.

Thermodynamic parameters					
Cr (VI)	**ΔH** (kj/kmol)	**ΔS** (kj/kmol)	**ΔG** (kj/mol)		
	39.92	0.147	25 ºC	35 ºC	45 ºC
			-4.298	-5.467	-7.273

Table 6. Reusing FA3 after desorption.

Cr (VI)	Removal efficiency (%)		
	First time application of FA3 after desorption	Second time application of FA3 after desorption	Third time application of FA3 after desorption
	81	76	69

Table 7. ARE, AARE and SD modeled by fuzzy for Cr (VI) removal efficiency.

Response variable	**Method**	**% ARE**	**% AARE**	**% SD**
Removal efficiency	Fuzzy	1.36	6.48	9.68

Table 8. Comparison between the method used in this study and other methods reported in the literatures.

Type of process	Experimental results (Maximum efficiency)	Method	Response variable	Statistical index	Ref.
Cr(VI) removal by ZVINs	> 88 %	ANN	Cr(VI) removal efficiency	R^2= 0.9803	[55]
Cd(II) removal by hematite	103 μmol/L	ANN and ANFIS	Cd(II) adsorption	R^2= 0.96 Average Errors < 1%	[56]
BOD removal by free-water surface (FWS)	> 98 %	Fuzzy	BOD and COD removal	R^2_{BOD}= 0.82 R^2_{COD}= 0.78	[57]
Lead removal by MEUF	> 99 %	Fuzzy	Permeate flux and the rejection rate	R^2 = 0.9185 R^2 = 0.9796	[58]
As(III) removal by Ce-HAHCl	> 98 %	ANN	As(III) removal prediction	R^2 = 0.975	[59]
Cr(VI) removal by DPOC	> 184 mg/g	ANN and RSM	Cr(VI) uptake tare	R^2_{ANN}= 0.99 R^2_{RSM}= 0.93	[60]
As(III) and Cr(VI) removal by ZEDA	97 % for As(III) 91 % for Cr(VI)	ANFIS	As(III) and Cr(VI) removal	$R^2_{As(III)}$= 0.94 $R^2_{Cr(VI)}$= 0.99	[61]
As(III) and As(V) removal by B. braunii biomass	> 85 % for As(III) > 88 % for As(V)	ANN	As(III) and As(V) removal	$R^2_{As(III)}$= 0.99 $R^2_{As(V)}$= 0.99	[62]
Adsorption of Cu(II) by pumice	> 98 %	ANN	Cu(II) removal	$R^2_{Cu(II)}$= 0.999	[63]
Cr(VI) removal by ZFA	> 90 %	ANN	Cr(VI) removal efficiency	R^2= 0.98	[64]
This study	> 84 %	Fuzzy	Cr(VI) removal efficiency	R^2= 0.9551	

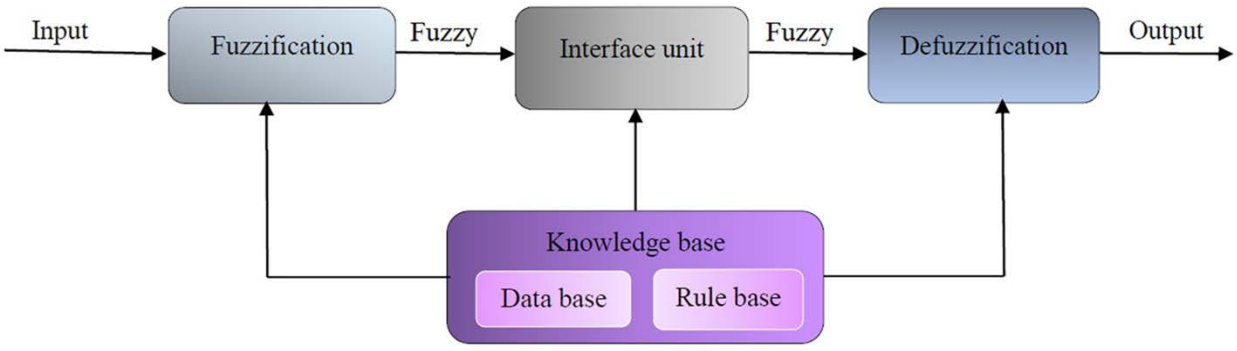

Fig. 1. Fuzzy inference system.

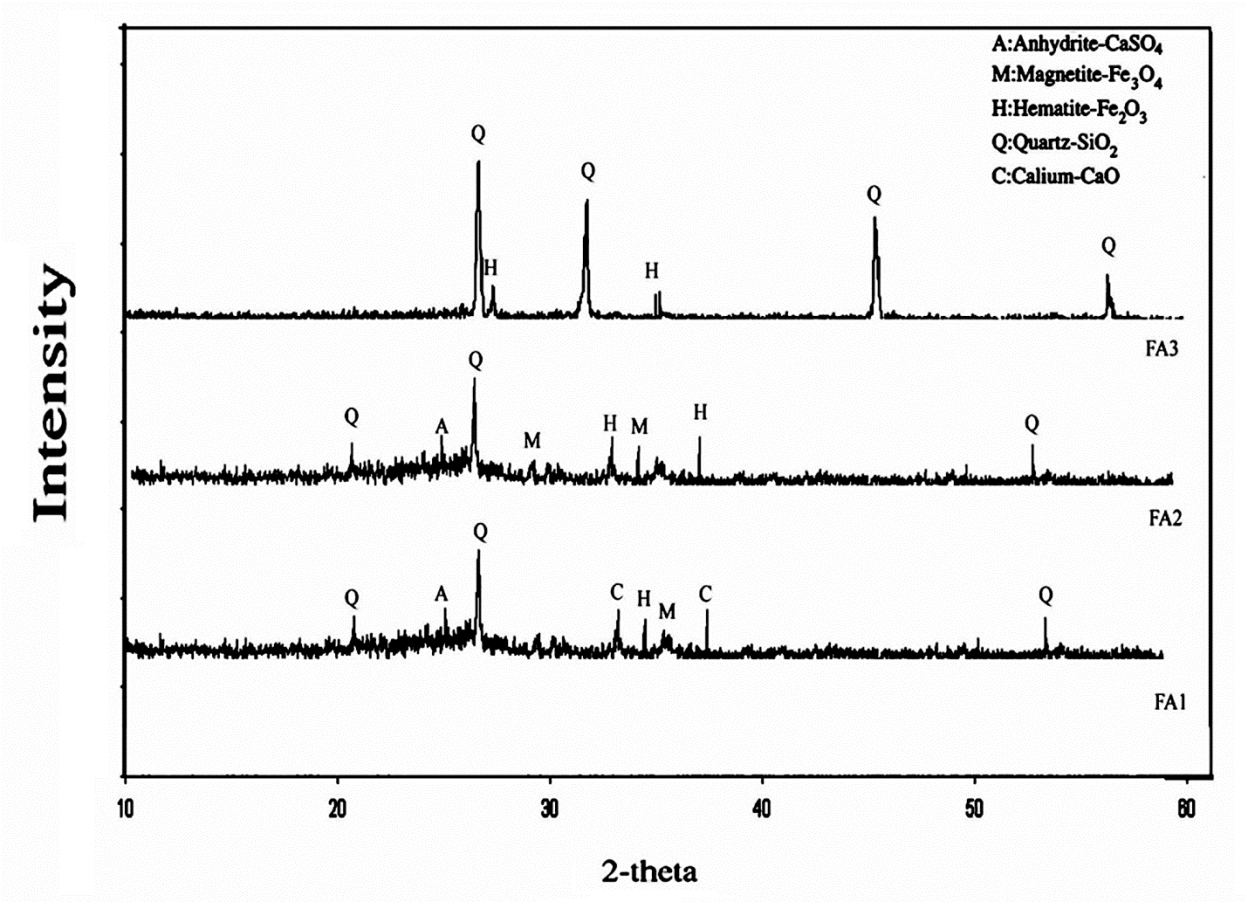

Fig. 2. X-ray diffraction patterns of FA1, FA2 and FA3

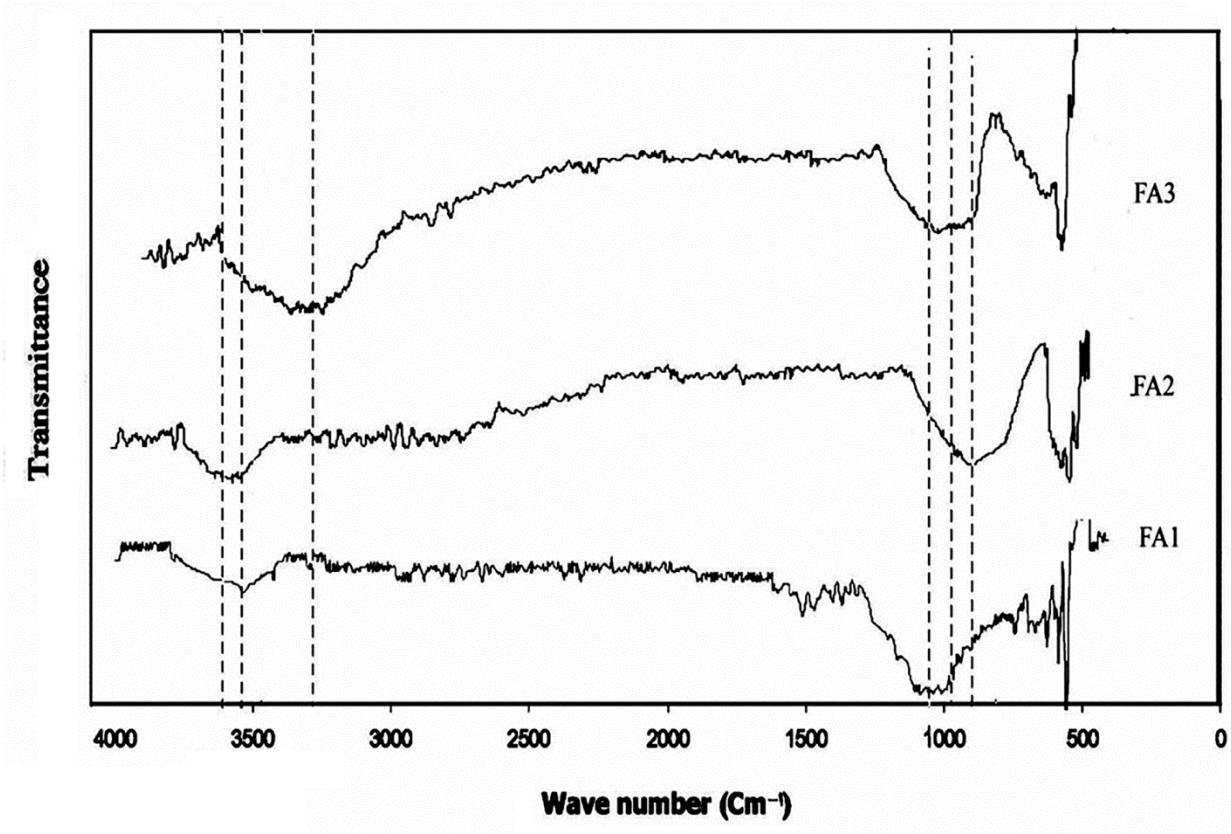

Fig. 3. FT-IR spectra of FA1, FA2 and FA3

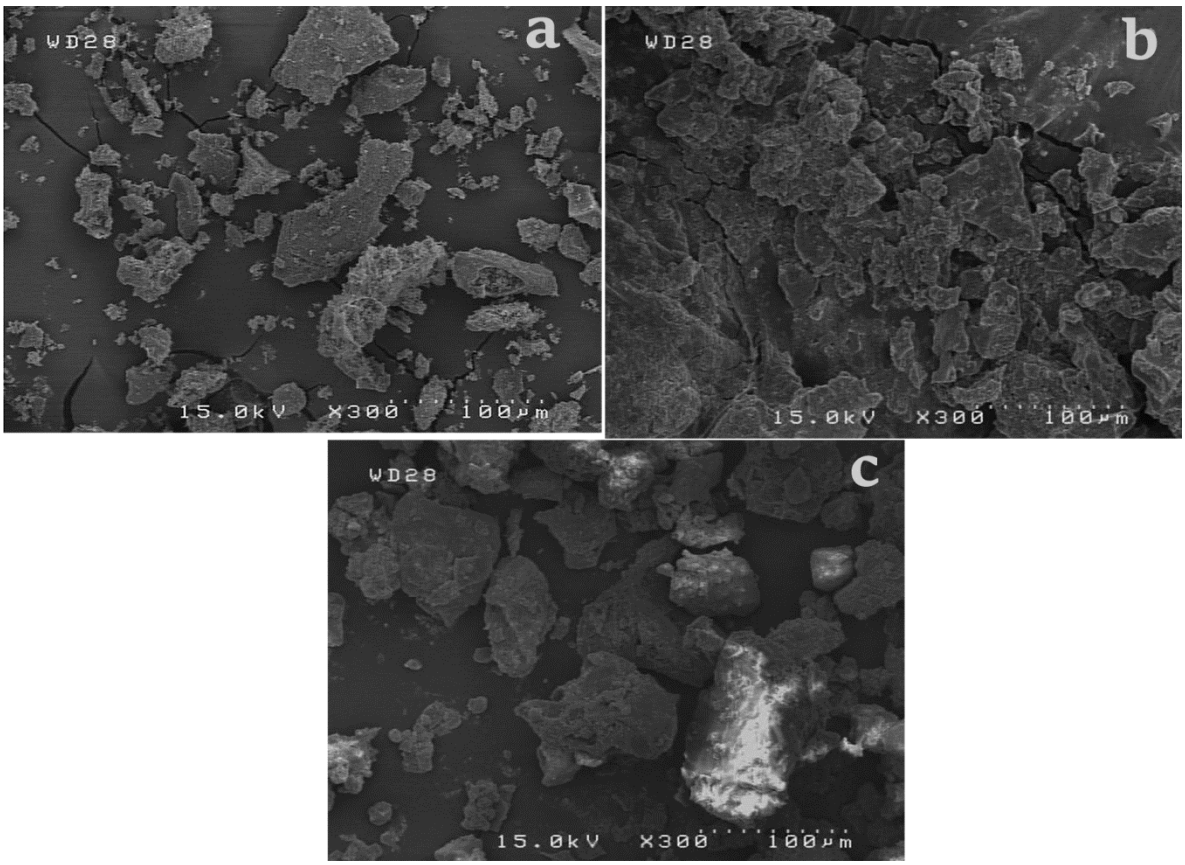

Fig. 4. SEM images of (a) FA1 (b) FA2 and (c) FA3

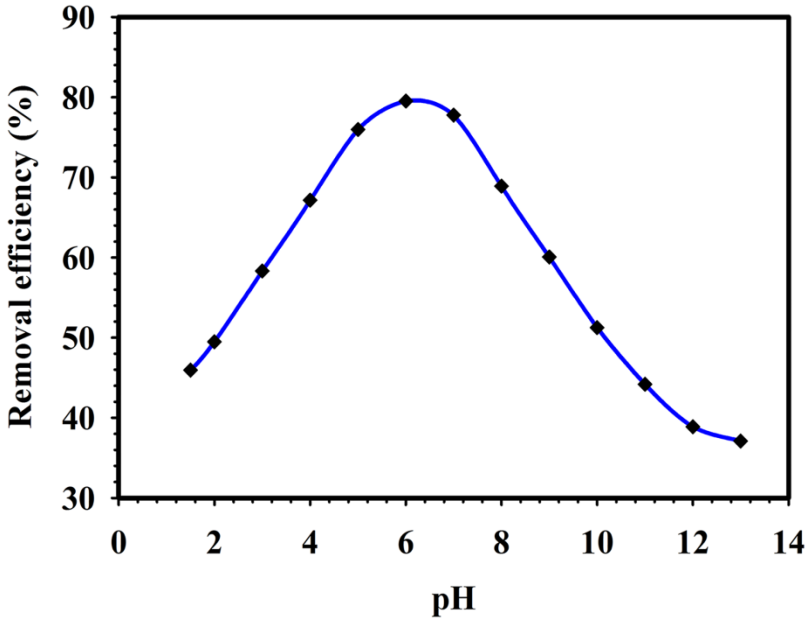

Fig. 5. Effect of pH on the Cr (VI) removal efficiency (Conditions: 53 mg/L initial Cr (VI) concentration, 250 rpm rotating speed, 10 h contact time, 25 mL solution volume and 2 g/L sorbent).

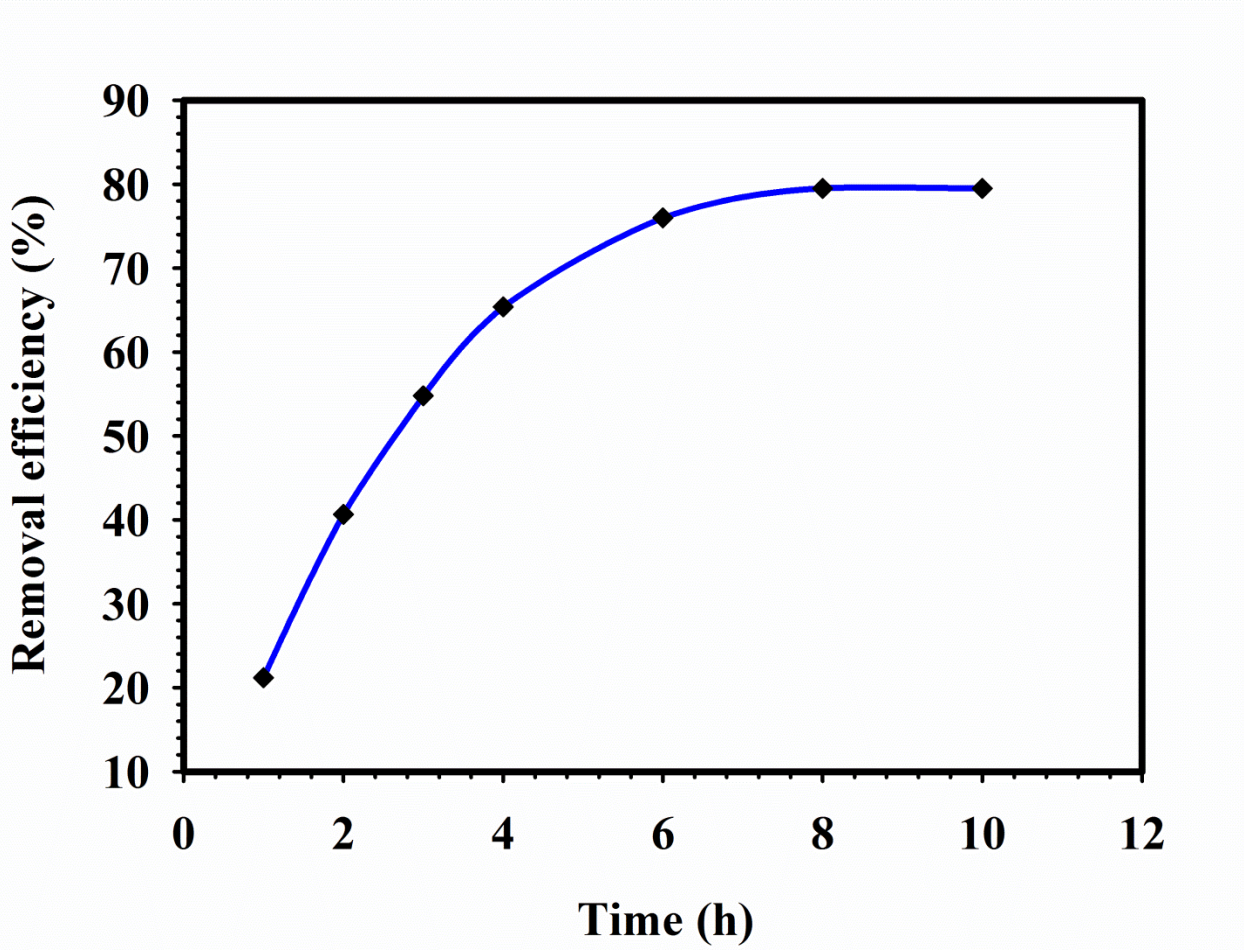

Fig. 6. Effect of contact time on Cr (VI) removal efficiency (Conditions: 53 mg/L initial Cr (VI) concentration, 250 rpm rotating speed, pH=8, 25 mL solution volume and 2 g/L sorbent).

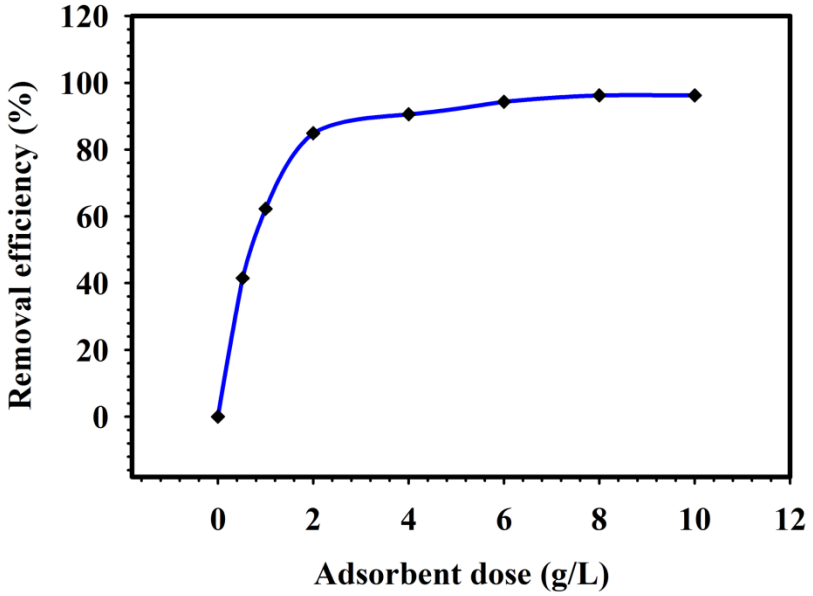

Fig. 7. Effect of sorbent dose on Cr (VI) removal efficiency (Conditions: 53 mg/L initial concentration, 250 rpm rotating speed, pH=8, 25 mL solution volume and 8 h contact time).

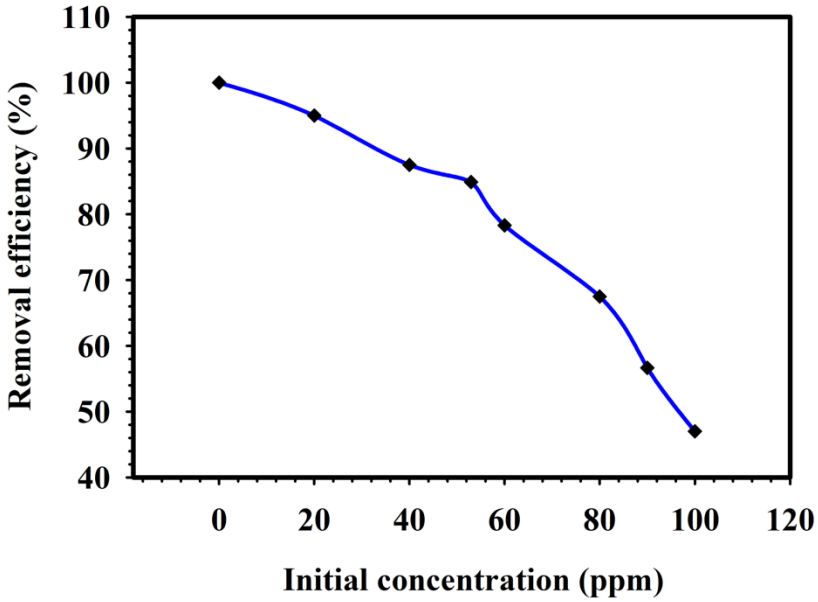

Fig. 8. Effect of initial concentration on Cr (VI) removal efficiency (Conditions: 2 g/L sorbent, 250 rpm rotating speed, pH=8, 25 mL solution volume and 8 h contact time).

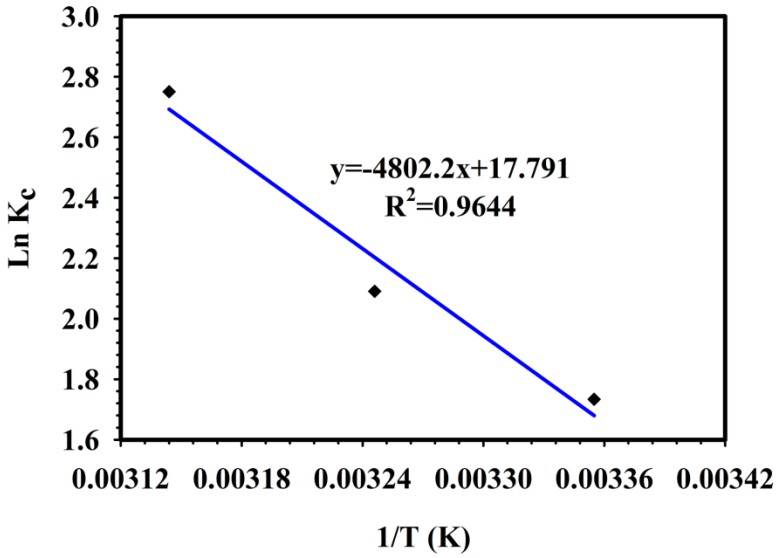

Fig. 9. Ln K_C versus 1/T for enthalpy and entropy changes of the sorption process.

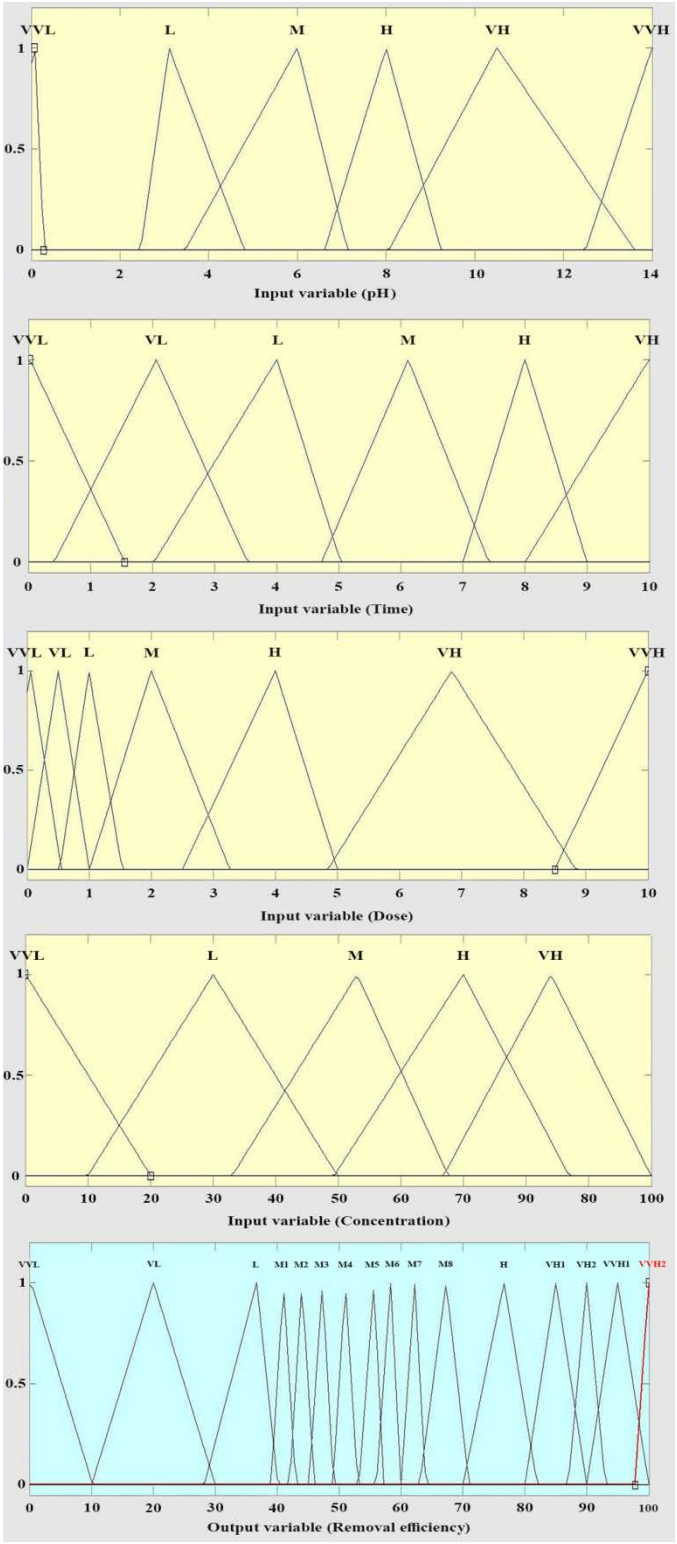

Fig. 10. Membership functions of input (pH, contact time, adsorbent dosage and initial Cr (VI) concentration) and output (Cr (VI) removal efficiency (%)) variables.

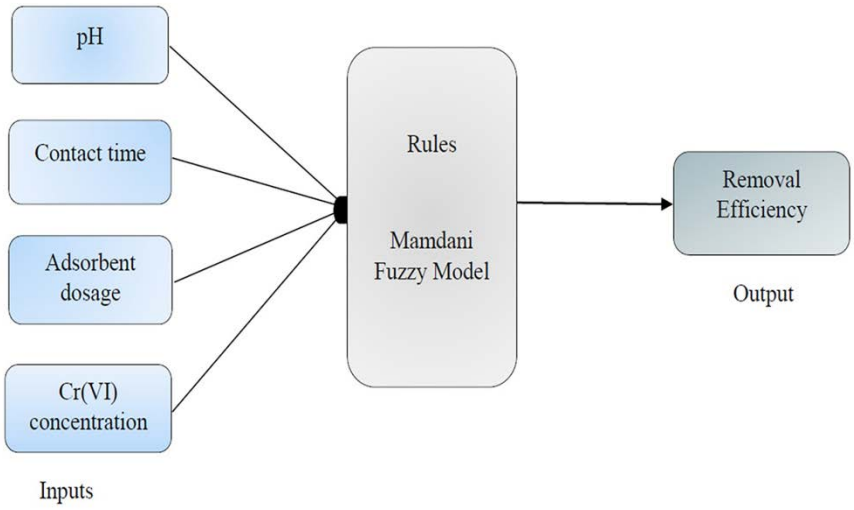

Fig. 11. Graphical representation of fuzzy model structure for Cr (VI) removal efficiency.

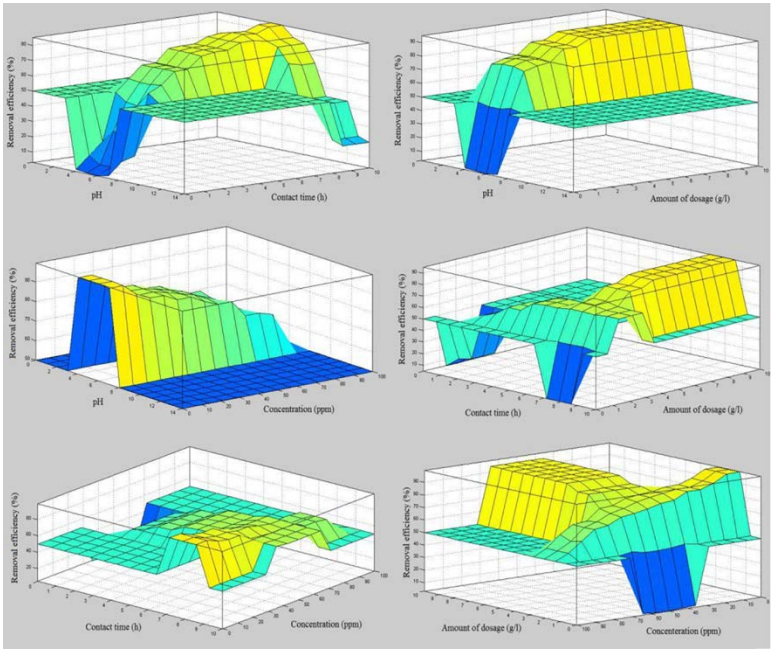

Fig. 12. Three-dimensional surfaces of fuzzy model rules for Cr (VI) removal efficiency (R %).

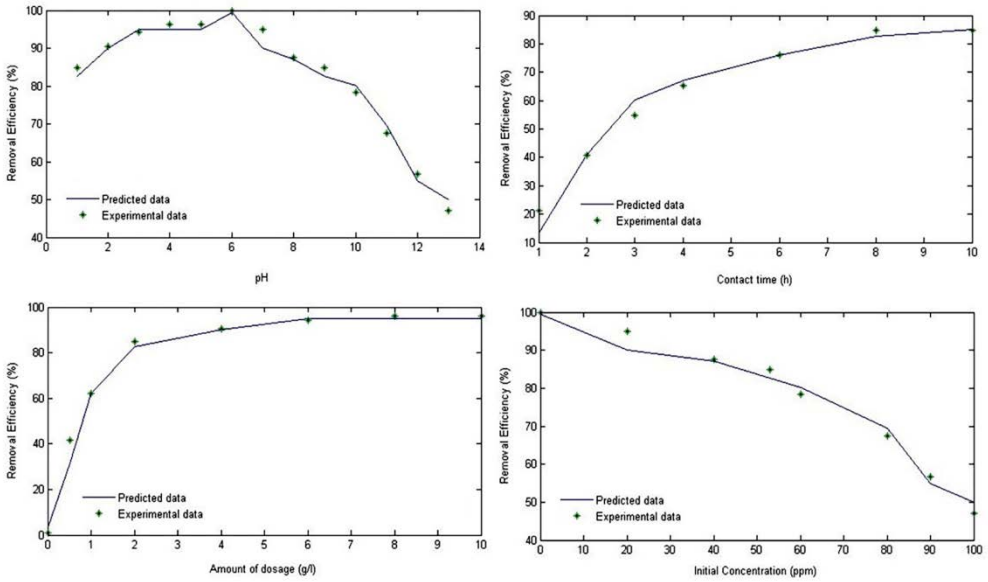

Fig. 13. Response of fuzzy inference model to Cr (VI) removal efficiency; (a) effect of pH, (b) effect of contact time, (c) effect of adsorbent dosage and (d) effect of initial Cr(VI) concentration.

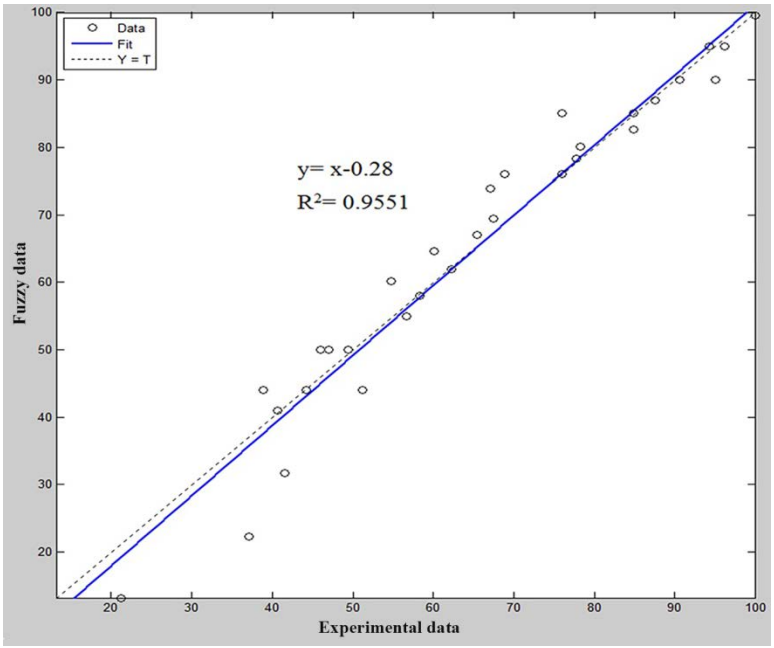

Fig. 14. Comparison of the experimental and predicted data for Cr (VI) removal efficiency.

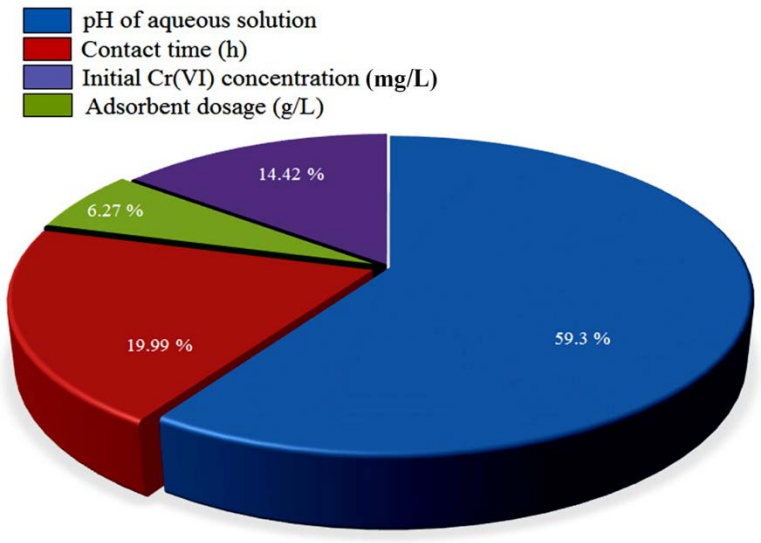

Fig. 15. Relative importance of each input variable on the Cr (VI) removal efficiency.